Impact of Ammonium Perchlorate Content on Electrically Controlled Gel Polymer Electrolyte Monopropellants

Harrison Autry,* Bradley Gobin,* Ryan Marks,† and Gregory Young‡
Virginia Polytechnic Institute and State University, Blacksburg, Virginia 24061
and
Afrida Anis,§ Prithwish Biswas,§ Keren Shi,§ Yujie Wang,§ and Michael R. Zachariah¶
University of California, Riverside, Riverside, California 92521

https://doi.org/10.2514/1.B39250

A group of five electrically controlled monopropellants were developed, and their fundamental rheological, electrochemical, thermal, and combustion properties were characterized. A baseline monopropellant was composed of lithium perchlorate complexed with polyethylene glycol to form an ionically conductive gel polymer electrolyte. Subsequent candidates were supplemented with varying amounts of ammonium perchlorate at a fixed polymer-to-oxidizer ratio to determine the effects of shifting oxidizer content on the fundamental properties. The ignition of the gel monopropellants using an applied DC voltage potential at atmospheric conditions was observed and determined to be primarily the result of an electrolytic reaction. Time-resolved infrared thermography confirmed initial heating and initiation of the gels at the cathode once temperatures had reached the decomposition temperature of the polymer. Fourier transform infrared analysis of collected residue from experiments halted before ignition revealed lithium deposition on the cathode, supporting electrochemical activity. It was found that the electrolytic ignition delay time was affected by the oxidizer content, the magnitude of the applied voltage, and the distance between the electrodes supplying the voltage.

I. Introduction

INTEREST and investments in the development of low-toxicity alternatives to the commonly used hydrazine monopropellant have increased considerably over recent years [1,2]. Simplified handling procedures and, in turn, lower storage and operating costs have been recognized as primary motivators for these desired advancements [1,2]. Potential candidates that have been developed and extensively researched in recent decades include ionic liquid monopropellants, such as those based on hydroxylammonium nitrate (HAN) and ammonium dinitramide (ADN) oxidizer salts [3,4]. Similar to hydrazine, these monopropellants have been demonstrated using catalytic and thermal ignition methods [5]. However, their ionic conductivity has led to interest in ignition by electrolytic means [6].

The HAN-based AF-M315E and the ADN-based FLP-106 and LMP-103S ionic liquid monopropellants have been researched as alternatives to hydrazine due to their desirable low toxicity, lower freezing point, density, and performance [4,7–10]. The use of catalysts such as iridium for ignition and sustained combustion with these monopropellants presents a challenge with temperature limitations and material selection [10–12]. Methods using catalysts and thermal conduction can have high temperature and energy requirements to achieve sustained combustion and regularly experience large heat loss, which becomes especially detrimental to ignition processes in small-scale systems due to their increased surface-to-volume ratio [6,13].

Decomposition by electrolysis, or applied voltage, is a method that can potentially decrease energy requirements in small-scale systems by lowering temperatures necessary to initiate the combustion process [14]. Studies have observed this phenomenon in HAN-based ionically conductive solutions where an applied electric potential initiated the electrochemical decomposition and subsequent ignition of the solution [6,8]. A study by Rahman et al. observed electrolytic decomposition of ADN in a similar manner, where a microsatellite propulsion system that minimized power requirements and ignition temperature was of primary interest [14]. It was also observed that the decomposition rate of the propellant is influenced by the magnitude of the applied voltage [14]. While previous work on electrolytic decomposition in propellants has been conducted with ionic liquids, there is reason to believe that ionically conducting gel monopropellants can utilize this phenomenon to avoid combustion inefficiencies while maintaining a gel's advantageous characteristics. Gel polymer electrolytes, or GPEs, are a group of materials that possess ion transport properties similar to those of ionic solutions [15]. As a result, they have the potential to utilize electrolysis in a similar fashion to HAN and ADN, where, in the right circumstance, decomposition followed by ignition of the gel can occur in an electrically controlled manner.

Gel propellants have also received past attention due to their combination of benefits inherited from traditional liquid and solid propellants, but not without drawbacks [16]. Benefits include stability in long-term storage, similar to solid propellants, as well as a throttleable aspect, which is a favorable feature of liquid rocket systems. Gel propellants perform comparably to liquids, achieving similar specific impulse; however, they can be enhanced with additives to increase their energy density [16]. Disadvantages are seen in combustion inefficiencies arising from low burn rates and difficulty achieving fine atomization. Due to their thixotropic behavior, the atomization of gels proves to be difficult without subjecting the propellant to increasing shear rates [17,18]. Since the 1990s, groups from Israel, Germany, and the United States have increased development and research in gel propellants for use in various applications extending from satellites to tactical missiles and gel-fueled ramjets [19,20]. Historically, studies on gel propulsion systems typically investigate liquid fuels with added gellants to increase viscosity and provide a matrix for the suspension of additives, such as metals and solid oxidizers. A study completed on gelled JP-8 droplet combustion suggested that the presence of unburned residual silica may play a

Presented as Paper 2023-2692 at the AIAA SciTech 2023 Forum, National Harbor, MD, January 23–May 27, 2023; received 5 May 2023; revision received 13 February 2024; accepted for publication 14 February 2024; published online 29 February 2024.

*Graduate Student, Department of Aerospace and Ocean Engineering.
†Undergraduate Student, Department of Aerospace and Ocean Engineering.
‡Associate Professor, Department of Aerospace and Ocean Engineering; gyoung1199@vt.edu (Corresponding Author).
§Graduate Student, Department of Chemical and Environmental Engineering, 900 University Avenue.
¶Professor, Department of Chemical and Environmental Engineering, 900 University Avenue.

role in nonuniform heating of the propellant, leading to combustion inefficiencies [18].

Gel polymer electrolytes are commonly researched for use in energy cells due to their ion transport properties [15,21]. This form of gel polymer electrolyte is created when an ionically conductive and viscous liquid polymer is combined with an ionic salt to form a complex. A common polymer investigated in this application is polyethylene glycol (PEG) due to its ability to be complexed with lithium salts [21]. The process of dissolving ionic salts in the polymer results in the salts breaking down into their corresponding anions and cations, which are responsive to an applied voltage potential. Electrically controllable gel propellants (ECGPs) are created as gel polymer electrolytes where the present ionic salt is also an oxidizer. A sufficient voltage application to the gel composition will cause the ions to flow to the electrodes, leading to decomposition and ignition [22].

Previous work on electrically controlled propellants (ECPs) by Gobin et al. has been completed to investigate the response of ionic oxidizers to a voltage application as well as to characterize the performance and combustion of both gel propellants using PEG and solid propellants using PEO as the respective polymers. In each instance, Gobin et al. demonstrated the dependence of ignition delay and regression rates on the magnitude of applied voltage [22–24]. Separate studies completed by Li et al. and Gnanaprakash et al. have also investigated the ignition of electrically controlled solid propellants (ECSPs) that utilize polyvinyl alcohol (PVA) as the polymer with metal additives at elevated pressures. It was found in both studies that increasing pressure and the presence of metal additives decreased ignition delay times by decreasing ignition energy requirements [25,26].

The following investigation focused on continuing the work completed by Gobin et al. with the development and characterization of fundamental properties of electrically controllable gel polymer electrolyte monopropellants [22]. Experiments were completed to characterize the ignition/combustion, mechanical, electrochemical, and thermal properties of five ECGPs as a function of the ratio of the propellant's oxidizer salts. Ignition/combustion aspects were investigated by observing ignition characteristics as a voltage potential is applied to the propellants, followed by a study completed with select propellants under varying pressures to describe their burn and extinction properties. Their mechanical and electrochemical properties were determined through rheological measurements and electrical impedance spectroscopy (EIS) studies, respectively, and the thermal characterization study was conducted to understand the thermal decomposition of the propellant constituents.

II. Methodology

A. Sample Preparation

The polymer used in this study was 400 $g \cdot mol^{-1}$ PEG sourced from Sigma-Aldrich, with oxidizer salts of ACS-grade lithium perchlorate (LP), sourced from Thermo Fisher Scientific with a minimum 95% purity, and ammonium perchlorate (AP) with a stated particle size of 200 microns from Pyro Chem Source. Lithium perchlorate was selected as the primary oxidizer alongside PEG due to the extensive research available on these components in GPE applications [21,27,28]. The monopropellants were prepared by dissolving the polymer in acetonitrile, which was sourced from Thermo Fisher Scientific with a minimum purity of 99.9%, and subsequently adding the oxidizer salts. The mixtures were stirred over heat while covered until the oxidizer salts were sufficiently dissolved, and then stirred uncovered to allow the solvent to evaporate and the mixtures to thicken. In the propellants that were supplemented with AP, it was observed that the larger AP particles do not fully dissolve, however, and are instead suspended in the gel matrix. The mixtures were further dried in a vacuum chamber, where they remained stored until experimentation to ensure no atmospheric moisture was absorbed.

The study was constrained by the burn characteristics of AP, for which controllability became a concern. An examination of an early propellant, which had an oxidizer composition of 50% AP and 50% LP as well as a polymer-to-oxidizer ratio of 1 : 3, resulted in a self-sustained flame, demonstrating that this would be an upper limit of AP present in the propellant. Thus, data collection began with a baseline propellant that utilized only LP as its oxidizer, and following iterations saw the incremental addition of AP. Theoretical values of flame temperature and specific impulse were calculated using NASA's Chemical Equilibrium with Applications (CEA) program [29]. The CEA program was used to find the peak for these values as a function of weight percent polymer in a PEG and LP propellant as well as a PEG and AP propellant using the equilibrium rocket problem with an assigned chamber pressure of 0.689 MPa and a supersonic area ratio of 100. The results of the calculations can be found in Fig. 1 below, which show that both the flame temperature and vacuum-specific impulse peak at 25% polymer mass for the LP and PEG compositions, while this occurs at 15% polymer mass for the AP and PEG compositions. Because of the focus of this research on the use of LP as the primary oxidizer, investigations proceeded with monopropellant candidates with a polymer content of 25% by mass. Figure 2 depicts the flame temperature and vacuum-specific impulse for a propellant composed of LP and PEG fixed at the selected polymer-to-oxidizer ratio as a function of increasing percent AP of the total oxidizer mass. Vertical black dashes on each represent the composition of the propellant candidates and are labeled as such, and Table 1 further details these candidates.

B. Ignition Characteristics

Experiments completed to characterize electrolytic ignition aspects consisted of extruding the monopropellants into the channel of a ceramic block, where they came into contact with parallel copper electrodes running the length of the block. A voltage was supplied to the electrodes via an XP HPT5K0-L DC power supply. This was done for a ceramic block with electrode gap widths of 0.635 cm for all propellant compositions as well as 0.318 cm for ECGP-4 to investigate ignition dependence on both applied voltage and electrode spacing. The propellants were fed into the ceramic block via a syringe that was loaded into a Harvard Apparatus PHD Ultra syringe pump. The syringe was outfitted with a ceramic tube at its exit to ensure the syringe pump was electrically isolated from the electrodes. The assembly was placed on top of a quartz window with a mirror situated

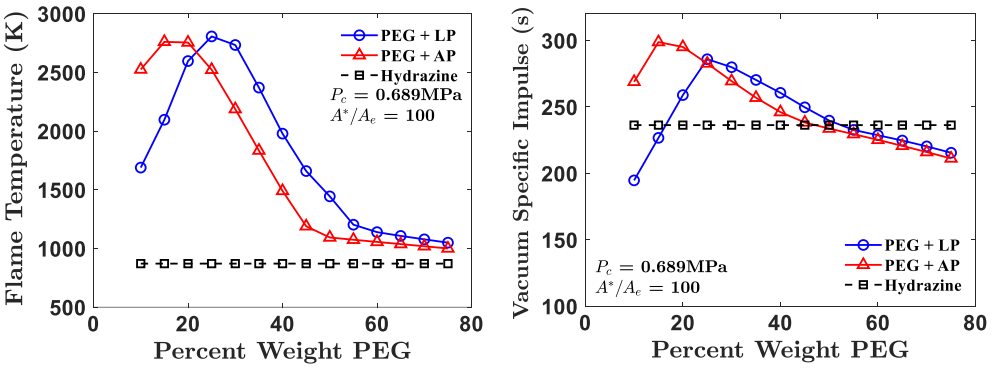

Fig. 1 Polymer weight percent vs flame temperature (top) and vacuum-specific (bottom) impulse for PEG+LP and PEG+AP compositions.

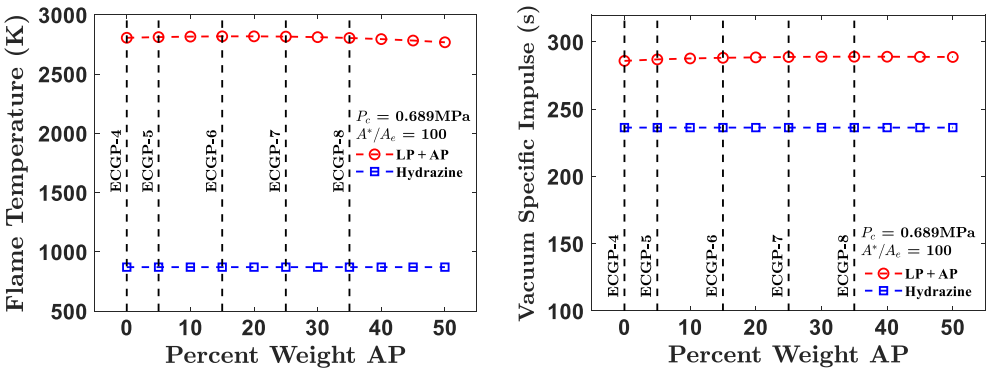

Fig. 2 AP weight percent of total oxidizer vs flame temperature (left) and specific impulse (right) at 25% weight polymer.

Table 1 Compositions of gel propellant candidates

Candidate name	%wt PEG	%wt LP	%wt AP
ECGP-4	25.00	75.00	0.00
ECGP-5	25.00	71.25	3.75
ECGP-6	25.00	63.75	11.25
ECGP-7	25.00	56.25	18.75
ECGP-8	25.00	48.75	26.25

underneath for a Vision Research Phantom VEO 7.10L high-speed camera to capture video. The experimental setup is visualized in Fig. 3, as detailed by Gobin et al. [22]. With a sufficient voltage applied to the electrodes, the gel begins to decompose and finally ignite. The ignition delay was characterized over a voltage range of 120–180 V in increments of 20 V. The ignition delay was defined as the time between a gel's first contact with the electrodes and the first light. With knowledge of the respective frames of these events and the sample frame rate of the camera, the ignition delay can be determined.

Additional static experiments were carried out in which a gel sample was placed between two electrodes while being monitored by a Telops FAST M3K high-speed infrared camera to capture the in-situ thermographs of the samples during the electrochemical reactions. A G4x microscope lens from Telops with a resolution of approximately 10 microns per pixel was used in this study. Residue collected from this experiment, along with the starting material, were analyzed using attenuated total reflectance–Fourier transform infrared (ATR-FTIR) on a Nicolet iS50R spectrometer equipped with a deuterated triglycine sulfate (DTGS) detector. The spectra were collected at a resolution of 4 cm^{-1}, and each spectrum consisted of 40 s cans that were averaged every 60 s. The data were processed using Happ-Genzel apodization, Mertz phase correction, and atmospheric suppression techniques.

C. Pressure Study

ECGP-4, ECGP-6, and ECGP-8 were selected to be studied under pressure in an optically accessible strand burner with a nitrogen purge to determine their pressure deflagration limit (PDL) and the corresponding burn rate. The propellants were placed in a sample carrier composed of a quartz tube with one end open and the other sealed by a 3D printed cap. A nichrome ignition wire was placed in contact with an igniter propellant, which rested on top of the propellant sample at the open end of the tube. The igniter was an AP composite solid propellant made in house and was composed of 65% by mass AP with a stated particle size of 200 microns, 10% AP with a stated particle size of 90 microns, both sourced from Pyro Chem Source; 17% hydroxyl-terminated polybutadiene (HTPB), with R-45 polymer and methylene diphenyl diisocyanate (MDI) curative sourced from RCS Rocket Motor Components, Inc.; and 8% H2 spherical aluminum powder sourced from Valimet, Inc., with a minimum purity of

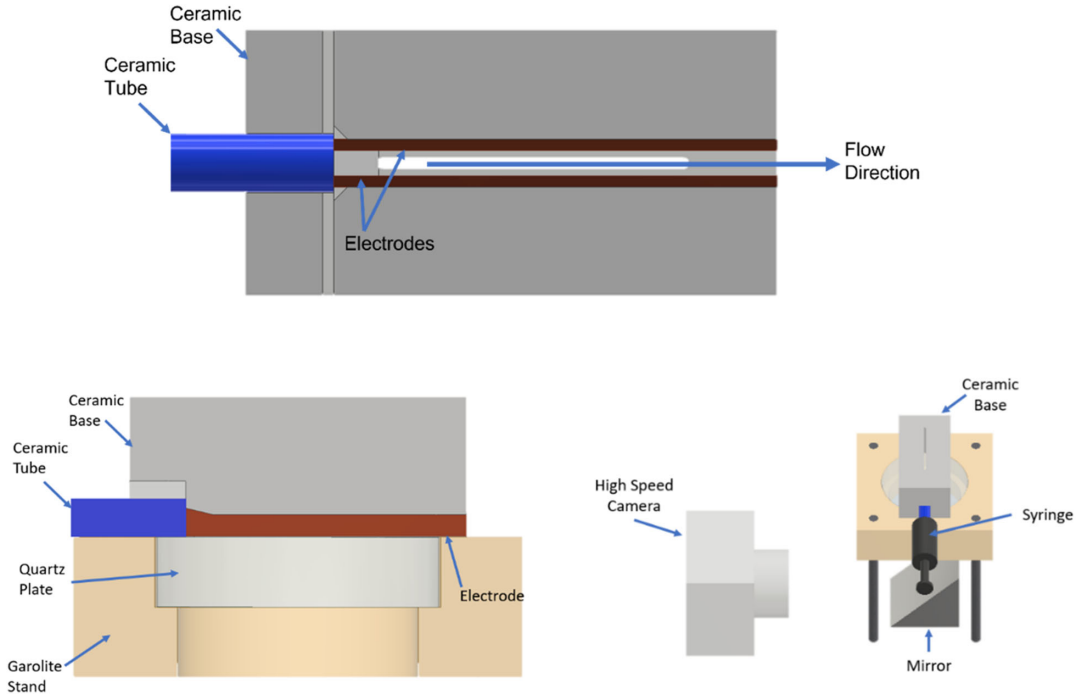

Fig. 3 Detailed apparatus setup [22], depicting bottom-up view (top), side-half-section view (left), and the experimental stand assembly (right).

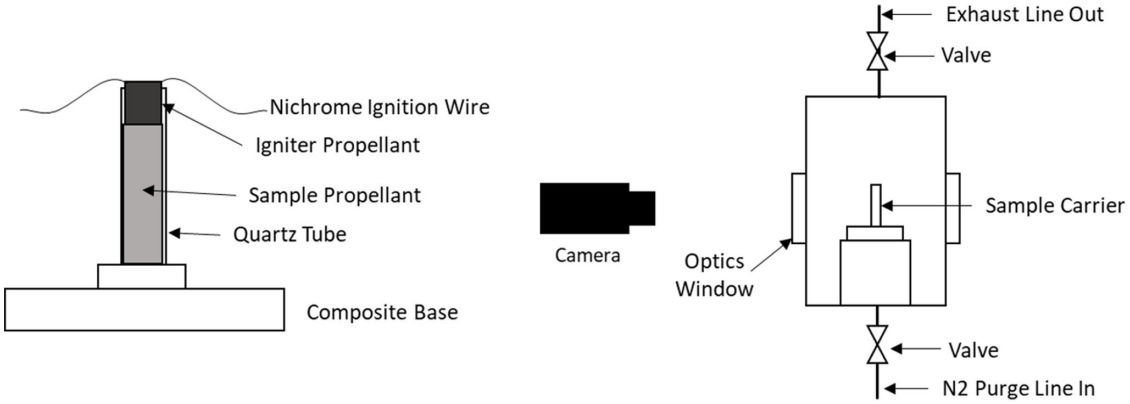

Fig. 4 Detailed view of strand burner sample carrier (left) and strand burner experimental setup (right).

99.7% and a particle size between two and three microns, per the supplier. The tube assembly was held in the strand burner by a flame-retardant fiberglass-epoxy composite base. The configuration is visually detailed in Fig. 4 below. The PDL and respective burn rates of ECGP-4, ECGP-6, and ECGP-8 were found as a result of this study.

III. Material Characterization

A. Rheological Characterization

A rheological study is necessary for all liquid and gel propellants to help understand their pumping requirements at expected operating temperatures. This was completed to observe the impact of varying oxidizer content on the flow properties of the ECGPs. Using a Discover HR-30 Rheometer with a 25 mm sandblasted parallel plate and a separation distance of 1000 microns, each propellant was subjected to rotational oscillations at angular frequencies ranging from 0.1 to 100 rad $\cdot$ s^{-1} and temperatures ranging from −20 to 20°C.

The results of the rheology study can be found in Fig. 5. For all ECGPs, viscosity increases with decreasing temperature. The gels displayed thixotropic behavior as their viscosity decreased with increasing applied angular velocity. At −20°C, it is shown that increasing AP content decreases the viscosity of the gels. This may in part be due to the replacement of dissolved LP with the suspension of partially dissolved AP particles in the matrix.

B. Electrochemical Impedance Spectroscopy

The electrochemical impedance spectroscopy (EIS) study was completed using an Autolab PGSTAT302N potentiostat to determine the resistivity of the gels. Data collected are used to explain the trends seen in the ignition delay study, as a gel with higher resistivity is expected to have a longer ignition delay. A small sample of each propellant was placed in an open-ended ceramic tube and contained between two cylindrical graphite electrodes inserted at both ends. The electrodes were then connected to the potentiostat, which applies an oscillating voltage potential to conduct electrochemical impedance measurements over a range of frequencies. The resulting measurements include the real and imaginary impedances, which are found by the potentiostat according to the applied voltage potential and current density reading, expressed as $\psi_s(t)$ and $j_s(t)$, respectively, in the following equations [30]:

$$\psi_s(t) = \psi_{DC} + \psi_0 e^{i2\pi ft} \tag{1}$$

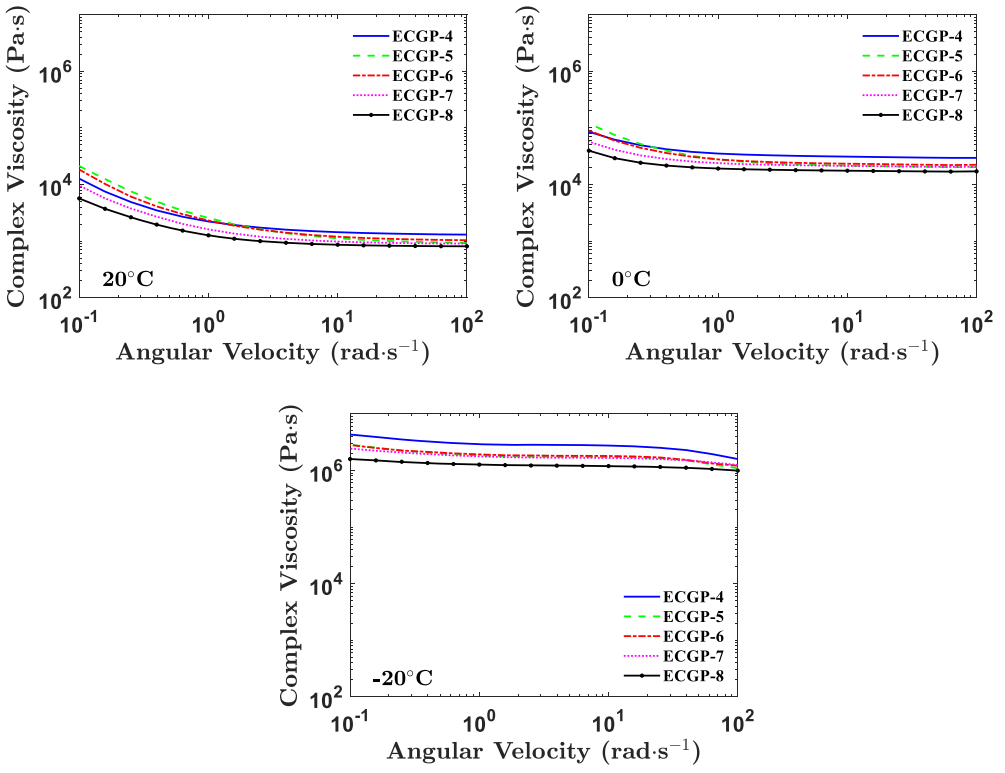

Fig. 5 Viscosity data for propellants at 20, 0, and −20°C (clockwise from top left).

$$j_s(t) = j_{DC} + j_0 e^{i[2\pi f t - \phi(f)]} \quad (2)$$

Here, ψ_{DC} and j_{DC} are the time-invariant DC voltage potential and current density, respectively; ψ_0 and j_0 are the time-invariant amplitudes of the oscillatory voltage and current density; and $\phi(f)$ is the phase angle between the applied voltage and current density reading as a function of frequency. The total electrochemical impedance Z can then be written in terms of its real and imaginary components, as well as the Euler formula in the following manner [31]:

$$Z = Z' + iZ'' = \frac{\psi_0}{j_0} * e^{i\phi(f)} \quad (3)$$

The imaginary component $-Z''$ can be plotted as a function of the real component Z' in a Nyquist plot, which depicts a semicircle over high frequencies followed by a linear relationship in the intermediate range of frequencies. An example for ECGP-6 is given in Fig. 6. The interior cusp of the graph occurs for the minimum imaginary impedance, which is a point at which the real impedance can be interpreted as the internal resistance of the gel [32].

The internal resistance is a property that is dependent on both the length and cross-sectional area of gel subject to the oscillating voltage; to use this data to describe the electrochemical properties of the gel, it is converted to resistivity using Eq. (4), where R is the measured real impedance, A is the cross-sectional area of the electrodes, and L is the length of the sample between electrodes. This measurement is a property that describes the ease of transportation of ions through the gels and is in units of ohmmeters.

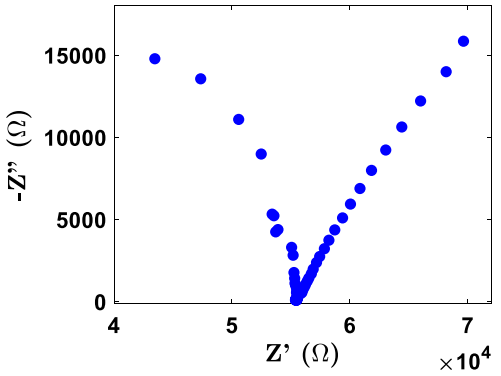

Fig. 6 Nyquist plot of ECGP-6.

Table 2 Average resistivity for ECGP compositions

Propellant	Average resistivity, Ω · m	Standard deviation
ECGP-4	225.57	10.0
ECGP-5	273.19	10.9
ECGP-6	325.59	10.7
ECGP-7	389.00	5.1
ECGP-8	485.43	7.4

$$\rho = \frac{RA}{L} \quad (4)$$

The results of the EIS study include the average resistivity and standard deviation over three experiments for each ECGP. The resistivity of a material is the reciprocal of its conductivity, meaning that materials with higher resistivity more strongly resist the transportation of ions within. These findings are reported in Table 2 and show that the average resistivity of the gels increased as AP content increased.

C. Thermal Characterization

Simultaneous thermogravimetric analysis/differential scanning calorimetry (TGA/DSC) was conducted using a Netzsch STA 449 F5 Jupiter TGA/DSC for the monopropellants and their individual constituents. The compositions were weighed and placed into an aluminum oxide crucible for experimentation. Each monopropellant sample was subjected to temperature increasing from 20 to 800°C at a heating rate of 10°C per minute with a continuous nitrogen purge.

The thermal decomposition data for the individual constituents of the ECGPs found in Fig. 7 are used to provide context to the results for the ECGPs, which are subsequently depicted in Fig. 8. In the constituents, AP is shown to have a notably lower thermal decomposition temperature than LP, which occurs at about 300°C as opposed to 500°C.

In the monopropellants, the initial mass loss between 90 and 160°C is attributed to acetonitrile that is retained in the gel. While the solvent has a boiling point of 82°C, it has been noted in studies that a bond forms between acetonitrile and ions, such as Li^+, prolonging its evaporation [33,34]. The onset of the primary exothermic peak for ECGP-4 occurs around 310°C and is seen to shift toward lower temperatures as AP is added. This is caused by the lower thermal decomposition temperature of AP displayed in Fig. 7, at which point it is able to react exothermically with the polymer fuel, leading to decreasing decomposition temperatures in the monopropellants as AP content increases. Lastly, the endothermic reaction that occurs above 600°C is attributed to the melting of lithium chloride, which is produced in the primary exothermic reaction of LP [35].

IV. Results and Discussion

A. Ignition Study

In the ignition study of the ECGPs, the gels are extruded along parallel electrodes, which apply the voltage from the power supply to the propellant. After being in contact with the electrodes for some time, the propellants begin to decompose into gases and ignite. Figure 9 is a sequence of images attained by high-speed cinematography depicting the ignition and combustion process of ECGP-6 with an applied voltage of 140 V. At time $t = 0$ s, the gel makes its initial contact with the electrodes. The gel advances through the channel and, at time $t = 13.2$ s, begins to decompose at the gel front, producing gases seen in the form of bubbles. Shortly thereafter, the gel ignites at time $t = 13.9$ s within the decomposition zone near the cathode. By time $t = 14.7$ s, a sustained flame is present. Additionally, Fig. 10

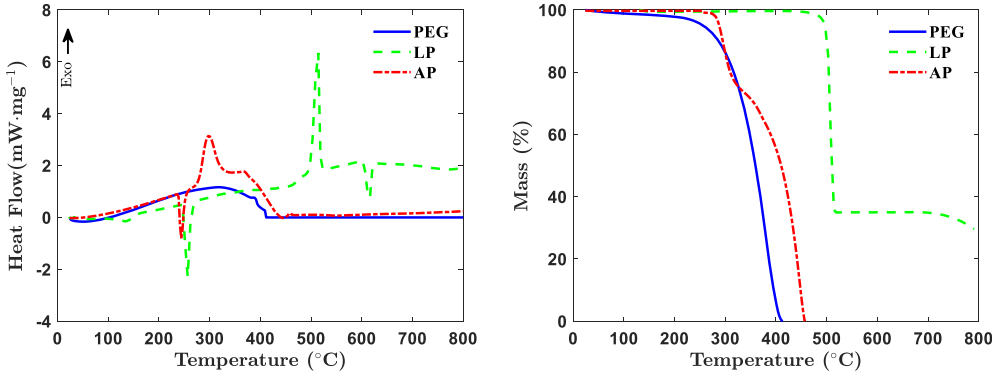

Fig. 7 DSC and TGA results for the constituents of ECGPs.

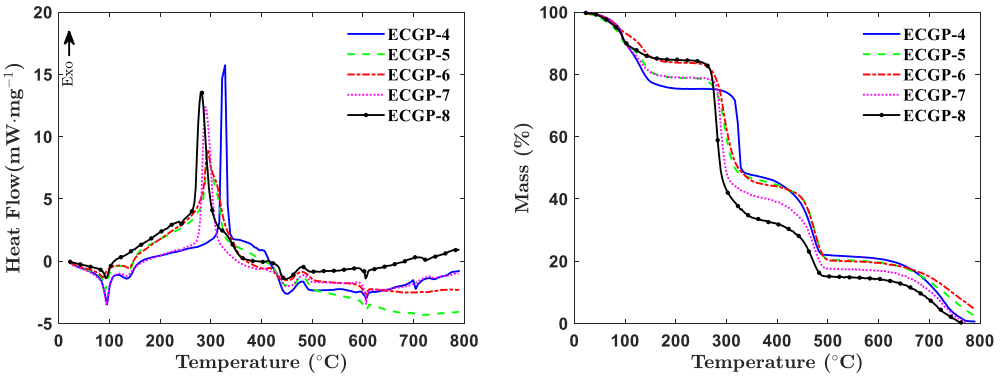

Fig. 8 DSC and TGA results for ECGPs.

Fig. 9 Electrically driven ignition and combustion of ECGP-6 at 140 V.

depicts the current draw of the same experiment, showing that current increases sharply once decomposition is achieved and peaks at the point of ignition.

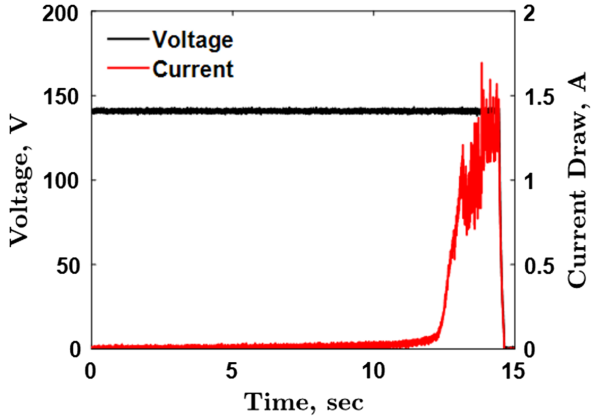

Fig. 10 Current draw during the electrolytically driven combustion of ECGP-6 at 140 V.

The results of the ignition study are depicted in Fig. 11, which shows the dependence of the ignition delay on the magnitude of the applied voltage for the different compositions as well as the dependence of the ignition delay on electrode spacing found for ECGP-4. The data points represented are the average times to ignition over at least three experiments, and the error bars represent the standard deviation.

Across all ECGPs, the ignition delay decreased with increasing applied voltage. ECGP-5 and ECGP-6 experienced less change in ignition delay as voltage changed, while ECGP-4 is shown to have had the highest sensitivity to changes in voltage. This can be expected, as ECGP-4 has the highest ionic conductivity. In the presence of small amounts of AP, the ignition delay is seen to decrease. However, as AP content continued to increase, the ignition delay increased across voltages. At 120 V, ECGP-4, ECGP-7, and ECGP-8 failed to ignite and only showed subtle signs of decomposition. Additionally, the ignition delay of ECGP-4 was found to decrease with decreasing electrode spacing, which is a result of increased current density, accelerating the electrolytic reaction [8].

The ignition of the gels is believed to be facilitated by competing thermal and electrochemical mechanisms. The applied voltage charges the GPE, causing the lithium cation to flow toward the cathode while the perchlorate anion flows to the anode. At the cathode, the cations are reduced, gaining an electron in an exothermic reaction. The oxidation of the perchlorate anion occurs at the anode, in which it loses an electron. The electrochemical mechanisms are described further in the study completed by Gobin et al. [22]. Ohmic heating exists in the presence of current and appears to contribute to the overall ignition process to varying degrees. If the propellants were only experiencing ohmic heating, the ignition of the gels would be facilitated in a similar manner to the previously discussed TGA and DSC results.

It is known that the Li^+ ions migrate to the cathode by hopping through the O-sites of PEG. The FTIR peaks associated with ClO_4 groups in $LiClO_4$/PEG are red shifted by 30 and 20 cm^{-1}, respectively, from their positions in bare $LiClO_4$, as shown in Fig. 12, verifying complexation of $LiClO_4$ and PEG. This indicates the weakening of the chlorine-oxygen bonds, which we attribute to the attractive interactions of Li^+ with the oxygen atoms in PEG. Such

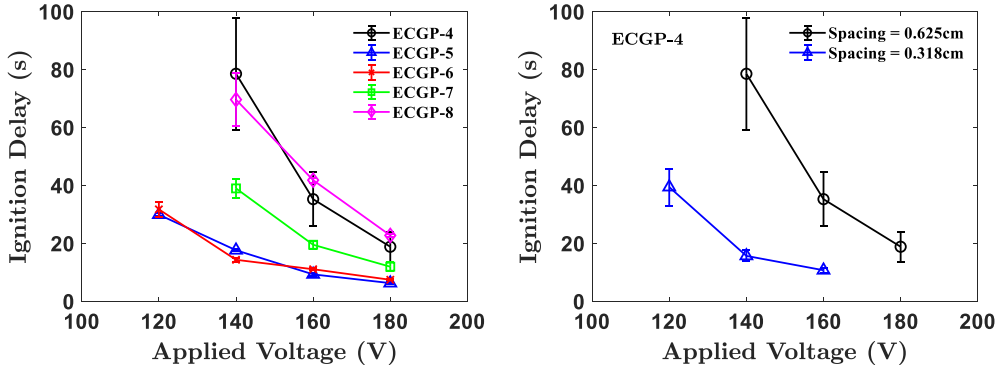

Fig. 11 Ignition delay for ECGPs as function of voltage (left) and electrode spacing (right).

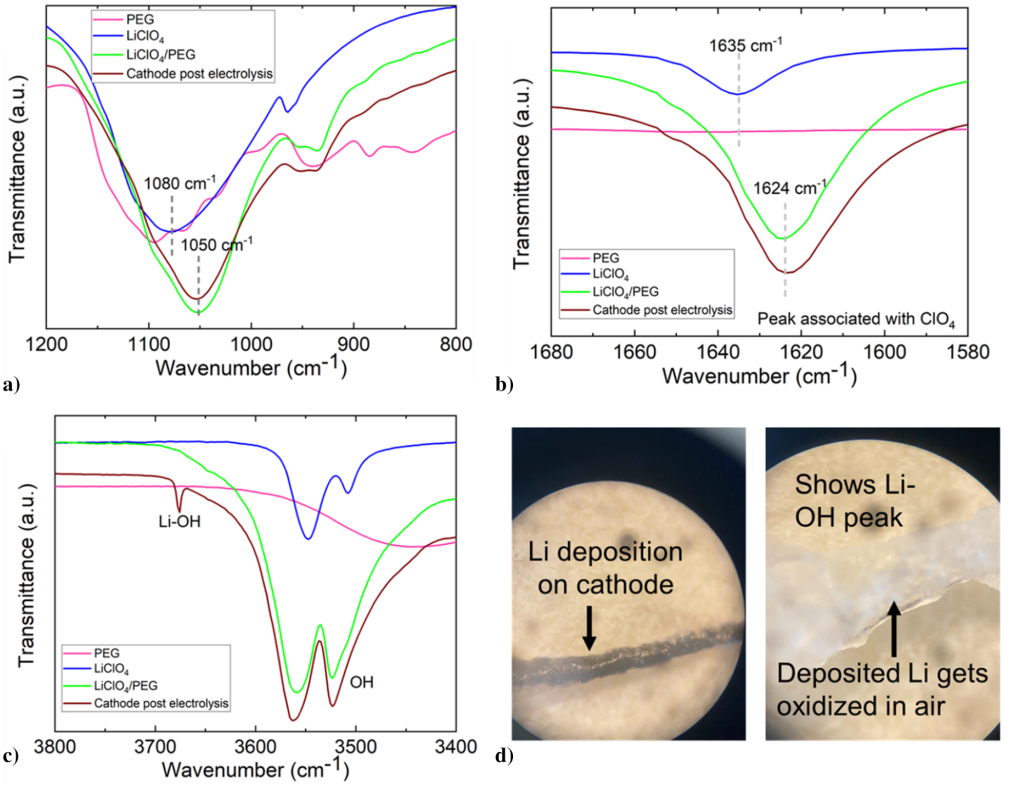

Fig. 12 FTIR peaks of ClO_4 in ECGP-4 redshifted by a) 30 cm^{-1} and b) 20 cm^{-1}; c) Li-OH peak of the cathode; and d) Li deposition.

complexation between the Li^+ and the O-groups of PEG will both promote gelation and the migration of Li^+ to the cathode. To analyze the products formed during the electrochemical reactions, the electrolysis process was stopped before the ignition event, and the cathode was characterized under an optical microscope and ATR-FTIR, which is shown in Fig. 12. Here, black Li deposition on the cathode is depicted, which becomes white upon prolonged exposure to the ambient atmosphere. The FTIR spectrum of the cathode with the white depositions shows a characteristic sharp peak of Li-OH, implying that Li is electrochemically reduced at the cathode, which, when exposed to air, is oxidized.

Figure 13 depicts infrared (IR) thermometry on the electrodes during the electrolysis process, showing that the cathode heats up first, leading to heat diffusion to the surroundings. Over time, the hotspot at the cathode reaches about 350°*C*, which is above the onset point of the exothermic reaction in ECGP-4, as shown in Fig. 8. Hence, it appears that the hotspot at the cathode initiates exothermic reactions, resulting in the ignition of ECGPs at the cathode.

B. Pressure Study

The combustion of ECGP-4, ECGP-6, and ECGP-8 was studied under pressure in an optically accessible strand burner with a nitrogen purge to determine the PDL and the corresponding burn rate for each. The burn rate was determined using a burn trajectory by measuring the distance that the center of the combustion front advanced toward the base of the sample carrier at multiple time intervals with knowledge of a reference distance $X_{ref} = 15.7$ mm. Figure 14 shows the regression of ECGP-8 at its determined PDL of 0.345 MPa. Time $t = 0$ s serves as a reference at which the igniter propellant had been consumed and the gel was first seen burning on its own. Between times $t = 15.3$ and $t = 61.1$ s, the combustion front of the gel regresses about 16.1 mm. Time $t = 61.1$ s shows the end of the propellant burn, at which point the gel is completely consumed.

The results of this study are recorded in Table 3. Because burn rate data were collected at the respective PDL of each monopropellant examined, these results are not directly comparable. Due to AP's enhancement of burn rate when paired with LP, it can be expected that an increase in AP content would lead to higher burn rates at any given pressure [36].

V. Conclusions

An investigation of the effects of the addition of ammonium perchlorate at a fixed polymer-to-oxidizer ratio on the material and

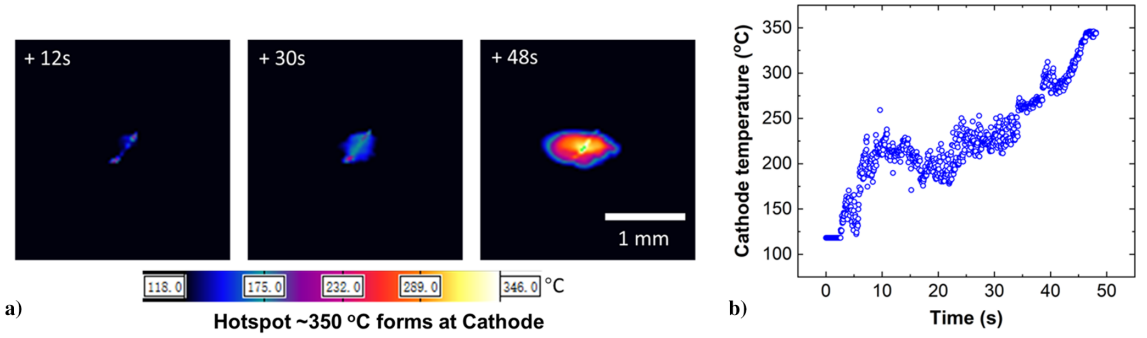

Fig. 13 a) Time-resolved IR thermograph shows hotspot formation at the cathode; b) temperature on the cathode increases until it reaches the ignition temperature of PEG.

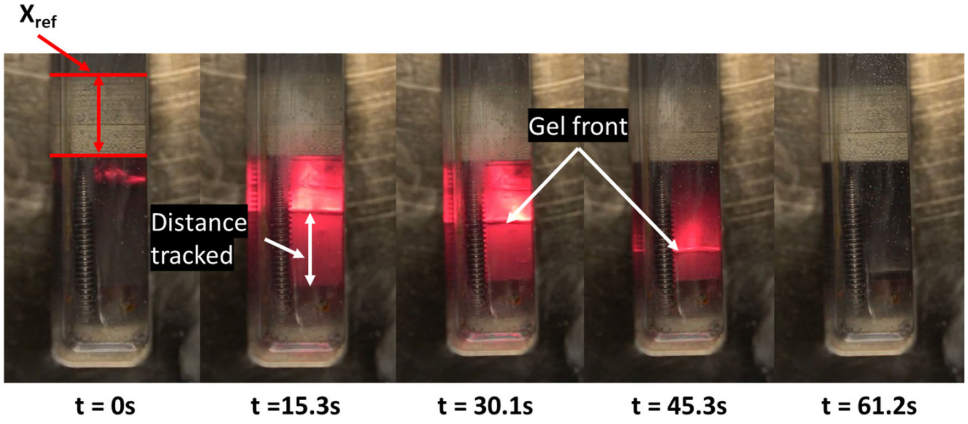

Fig. 14 Regression of ECGP-8 at 0.345 MPa.

Table 3 Pressure deflagration limit and corresponding regression rate for select candidates

Candidate name	Pressure deflagration limit, MPa	Regression rate at PDL, mm/s	Standard deviation
ECGP-4	2.41	0.637	0.13
ECGP-6	1.03	0.896	0.11
ECGP-8	0.345	0.357	0.0077

combustion properties of an electrically controlled monopropellant composed of a gel polymer electrolyte was completed. Due to their ionic conductivity, the gel monopropellants are able to use electrolytic mechanisms to decompose and ignite with an applied voltage potential.

Material properties that were characterized include the monopropellants' rheology as a function of temperature, their conductivity in an EIS study, and their thermal decomposition using simultaneous TGA/DSC. It was found that increasing the AP content decreased the viscosity of the gels. Increases in AP content also led to a decrease in ionic conductivity, which had a direct impact on ignition delay. The primary thermal decomposition temperature decreased with an increased presence of AP, reflecting the lower decomposition of AP when compared to LP and its exothermic reaction with the polymer fuel. The material properties were further used to understand the combustion characteristics of the monopropellants.

The ignition delay of the monopropellants was shown to be sensitive to oxidizer content, voltage magnitude, and electrode spacing. As the conductivity of the gels decreased, electrolysis was slowed, and the ignition delay was prolonged. This indicates that the ignition of the gels with an applied voltage was characterized by competing electrochemical and thermal processes. Additionally, both the increase in applied voltage magnitude and the decrease in electrode spacing were shown to enhance the electrolysis of the gels, facilitating their ignition. Finally, at elevated pressures, the increase in AP content was shown to decrease the PDL of the gels.

Acknowledgments

The authors from Virginia Polytechnic Institute and State University are grateful for the support of Mitat Birkan of the Air Force Office of Scientific Research under grant FA9550-21-1-0265. The authors of the University of California, Riverside, were supported by an Office of Naval Research grant (Chad Stoltz). In addition, the authors gratefully acknowledge the help of Grant Risha of Penn State Altoona for providing support in the design of the strand burner. This work was made possible by the use of Virginia Tech's Materials Characterization Facility, which is supported by the Institute for Critical Technology and Applied Science, the Macromolecules Innovation Institute, and the Office of the Vice President for Research and Innovation.

References

[1] Morgan, O. M., and Meinhardt, D. S., "Monopropellant Selection Criteria—Hydrazine and Other Options," *35th Joint Propulsion Conference and Exhibit*, AIAA Paper 1999-2595, June 1999. https://doi.org/10.2514/6.1999-2595

[2] Sackheim, R. L., and Masse, R. K., "Green Propulsion Advancement: Challenging the Maturity of Monopropellant Hydrazine," *Journal of Propulsion and Power*, Vol. 30, No. 2, 2014, pp. 265–276. https://doi.org/10.2514/1.B35086

[3] Gohardani, A. S., Stanojev, J., Demairé, A., Anflo, K., Persson, M., Wingborg, N., and Nilsson, C., "Green Space Propulsion: Opportunities and Prospects," *Progress in Aerospace Sciences*, Vol. 71, Nov. 2014, pp. 128–149. https://doi.org/10.1016/j.paerosci.2014.08.001

[4] Freudenmann, D., and Ciezki, H. K., "ADN and HAN-Based Monopropellants—A Minireview on Compatibility and Chemical Stability in Aqueous Media," *Propellants, Explosives, Pyrotechnics*, Vol. 44, No. 9, 2019, pp. 1084–1089. https://doi.org/10.1002/prep.201900127

[5] Amrousse, R., Hori, K., Fetimi, W., and Farhat, K., "HAN and ADN as Ionic Liquid Monopropellants: Thermal and Catalytic Decomposition Processes," *Applied Catalysis B: Environmental*, Vol. 127, Oct. 2012, pp. 121–128. https://doi.org/10.1016/j.apcatb.2012.08.009

[6] Risha, G. A., Yetter, R. A., and Yang, V., "Electrolytic-Induced Decomposition and Ignition of HAN-Based Liquid Monopropellants," *International Journal of Energetic Materials and Chemical Propulsion*, Vol. 6, No. 5, 2007, pp. 575–588. https://doi.org/10.1615/IntJEnergeticMaterialsChemProp.v6.i5.30

[7] Hawkins, T. W., Brand, A. J., McKay, M. B., and Tinnirello, M., "Reduced Toxicity, High Performance Monopropellant at the U.S. Air Force Research Laboratory," Air Force Research Lab., AFRL-RZ-ED-TP-2010-219, Huntsville, AL, May 2010.

[8] Khare, P., Yang, V., Meng, H., Risha, G. A., and Yetter, R. A., "Thermal and Electrolytic Decomposition and Ignition of HAN-Water Solutions," *Combustion Science and Technology*, Vol. 187, No. 7, 2015, pp. 1065–1078. https://doi.org/10.1080/00102202.2014.993033

[9] Larsson, A., and Wingborg, N., "Green Propellants Based on Ammonium Dinitramide (ADN)," *Advances in Spacecraft Technologies*, InTech, Croatia, 2011, pp. 139–154. https://doi.org/10.5772/568

[10] Wilhelm, M., Negri, M., Ciezki, H., and Schlechtriem, S., "Preliminary Tests on Thermal Ignition of ADN-Based Liquid Monopropellants," *Acta Astronautica*, Vol. 158, May 2019, pp. 388–396. https://doi.org/10.1016/j.actaastro.2018.05.057

[11] Amrousse, R., Katsumi, T., Niboshi, Y., Azuma, N., Bachar, A., and Hori, K., "Performance and Deactivation of IR-Based Catalyst During Hydroxylammonium Nitrate Catalytic Decomposition," *Applied Catalysis A: General*, Vol. 452, Feb. 2013, pp. 64–68. https://doi.org/10.1016/j.apcata.2012.11.038

[12] Courthéoux, L., Amariei, D., Rossignol, S., and Kappenstein, C., "Thermal and Catalytic Decomposition of HNF and HAN Liquid Ionic as Propellants," *Applied Catalysis B: Environmental*, Vol. 62, Nos. 3–4, 2006, pp. 217–225. https://doi.org/10.1016/j.apcatb.2005.07.016

[13] Wu, M., and Yetter, R. A., "A Novel Electrolytic Ignition Monopropellant Microthruster Based on Low Temperature Co-Fired Ceramic Tape

Technology," *Lab on a Chip*, Vol. 9, No. 7, 2009, pp. 910–916. https://doi.org/10.1039/B812737A

[14] Rahman, A., Chin, J., Kabir, F., and Hung, Y. M., "Characterization and Thrust Measurements from Electrolytic Decomposition of Ammonium Dinitramide (ADN) Based Liquid Monopropellant FLP-103 in MEMS Thrusters," *Chinese Journal of Chemical Engineering*, Vol. 26, No. 9, 2018, pp. 1992–2002. https://doi.org/10.1016/j.cjche.2017.09.016

[15] Stephan, A. M., "Review on Gel Polymer Electrolytes for Lithium Batteries," *European Polymer Journal*, Vol. 42, No. 1, 2006, pp. 21–42. https://doi.org/10.1016/j.eurpolymj.2005.09.017

[16] Natan, B., and Rahimi, S., "The Status of Gel Propulsion in Year 2000," *International Journal of Energetic Materials and Chemical Propulsion*, Vol. 5, Nos. 1–6, 2002, pp. 172–194. https://doi.org/10.1615/IntJEnergeticMaterialsChemProp.v5.i1-6.200

[17] Nachmoni, G., and Natan, B., "Combustion Characteristics of Gel Fuels," *Combustion Science and Technology*, Vol. 156, No. 1, 2000, pp. 139–157. https://doi.org/10.1080/00102200008947300

[18] Arnold, R., and Anderson, W., "Droplet Burning of JP-8/Silica Gels," *48th AIAA Aerospace Sciences Meeting Including the New Horizons Forum and Aerospace Exposition*, AIAA Paper 2010-0421, Jan. 2010. https://doi.org/10.2514/6.2010-421

[19] Ciezki, H. K., Naumann, K. W., and Weiser, V., "Status of Gel Propulsion in the Year 2010 with a Special View on the German Activities," Deutscher Luft- und Raumfahrtkongress, Hamburg, Germany, 2010.

[20] Natan, B., and Hasan, D., "Advances in Gel Propulsion," *International Journal of Energetic Materials and Chemical Propulsion*, Vol. 18, No. 4, 2019, pp. 303–323. https://doi.org/10.1615/IntJEnergeticMaterialsChemProp.2019028375

[21] Xue, Z., He, D., and Xie, X., "Poly(ethylene oxide)-Based Electrolytes for Lithium-Ion Batteries," *Journal of Materials Chemistry A*, Vol. 3, No. 38, 2015, pp. 19,218–19,253. https://doi.org/10.1039/C5TA03471J

[22] Gobin, B., Harvey, N., Arnold, C., Whalen, S., and Young, G., "Utilization of Ionically Conducting Polymers in Electrically Controlled Gel Monopropellants," *Journal of Propulsion and Power*, Vol. 38, No. 6, 2022, pp. 1017–1024. https://doi.org/10.2514/1.B38748

[23] Gobin, B., Harvey, N., and Young, G., "Combustion Characteristics of Electrically Controlled Solid Propellants Using Polymer Electrolytes," *Combustion and Flame*, Vol. 244, Oct. 2022, Paper 112291. https://doi.org/10.1016/j.combustflame.2022.112291

[24] Gobin, B., Reiter, P., Whalen, S., and Young, G., "Extinguishing and Reignition Characteristics of Electrically Controllable Solid Propellants Under Elevated Pressures," *Journal of Propulsion and Power*, Vol. 40, No. 1, 2024, pp. 152–163. https://doi.org/10.2514/1.B39189

[25] Gnanaprakash, K., Lim, D., and Yoh, J. J., "Combustion Characteristics of Lithium Perchlorate-Based Electrically Controlled Solid Propellants at Elevated Pressures," *Thermochimica Acta*, Vol. 720, Feb. 2023, Paper 179421. https://doi.org/10.1016/j.tca.2022.179421

[26] Li, Y., Xia, Z., Ma, L., and Na, X., "Ignition and Extinction Characteristics of Electrically Controlled Solid Propellants," *Journal of Propulsion and Power*, Vol. 39, No. 3, 2023, pp. 340–350. https://doi.org/10.2514/1.B38807

[27] Li, W., Pang, Y., Liu, J., Liu, G., Wang, Y., and Xia, Y., "A PEO-Based Gel Polymer Electrolyte for Lithium Ion Batteries," *RSC Advances*, Vol. 7, No. 38, 2017, pp. 23,494–23,501. https://doi.org/10.1039/C7RA02603J

[28] Mao, G., Saboungi, M.-L., Price, D. L., Badyal, Y. S., and Fischer, H. E., "Lithium Environment in PEO-LiClO4 Polymer Electrolyte," *Europhysics Letters*, Vol. 54, No. 3, 2001, pp. 347–353. https://doi.org/10.1209/epl/i2001-00249-7

[29] Gordon, S., and McBride, B. J., "Computer Program for Calculation of Complex Chemical Equilibrium Compositions and Applications," NASA RP-1311, 1994.

[30] Careem, M. A., Noor, I. S. M., and Arof, A. K., "Impedance Spectroscopy in Polymer Electrolyte Characterization," *Characterization Techniques and Energy Applications*, Wiley–VCH Verlag GmbH & Co., Weinheim, Germany, 2020, pp. 23–64.

[31] Mei, B., Munteshari, O., Lau, J., Dunn, B., and Pilon, L., "Physical Interpretations of Nyquist Plots for EDLC Electrodes and Devices," *Journal of Physical Chemistry C*, Vol. 122, No. 1, 2018, pp. 194–206. https://doi.org/10.1021/acs.jpcc.7b10582

[32] Lei, C., Markoulidiz, F., Ashitaka, Z., and Lekakou, C., "Reduction of Porous Carbon/Al Contact Resistance for an Electric Double-Layer Capacitor (EDLC)," *Electrochimica Acta*, Vol. 92, March 2013, pp. 183–187. https://doi.org/10.1016/j.electacta.2012.12.092

[33] Commarieu, B., Paolella, A., Collin-Martin, S., Gagnon, C., Vijh, A., Guerfi, A., and Zaghib, K., "Solid-to-Liquid Transition of Polycarbonate Solid Electrolytes in Li-Metal Batteries," *Journal of Power Sources*, Vol. 436, Oct. 2019, Paper 226852. https://doi.org/10.1016/j.jpowsour.2019.226852

[34] O'Donnell, J. F., Ayres, J. T., and Mann, C. K., "Preparation of High Purity Acetonitrile," *Analytical Chemistry*, Vol. 37, No. 9, 1965, pp. 1161–1162. https://doi.org/10.1021/ac60228a027

[35] Markowitz, M. M., Boryta, D. A., and Stewart, H., "Lithium Perchlorate Oxygen Candle. Pyrochemical Source of Pure Oxygen," *Industrial & Engineering Chemistry Product Research and Development*, Vol. 3, No. 4, 1964, pp. 321–330. https://doi.org/10.1021/i360012a016

[36] Gobin, B., Whalen, S., Plunkett, E. M., Godshall, G. F., Moore, R. B., and Young, G., "Effect of Electrical Stimuli on Combustion Behavior of Solid Oxidizers," *International Journal of Energetic Materials and Chemical Propulsion*, Vol. 20, No. 3, 2021, pp. 27–44. https://doi.org/10.1615/IntJEnergeticMaterialsChemProp.2021038286

L. Maurice
Associate Editor